JACS
JOURNAL OF THE AMERICAN CHEMICAL SOCIETY
Article
pubs.acs.org/JACS

Structure of Colloidal Quantum Dots from Dynamic Nuclear Polarization Surface Enhanced NMR Spectroscopy

Laura Piveteau,[†,‡] Ta-Chung Ong,[†] Aaron J. Rossini,[§] Lyndon Emsley,[*,§] Christophe Copéret,[*,†] and Maksym V. Kovalenko[*,†,‡]

[†]Department of Chemistry and Applied Biosciences, ETH Zürich, Vladimir Prelog Weg 1-5, Zürich CH-8093, Switzerland
[‡]Empa-Swiss Federal Laboratories for Materials Science and Technology, Überlandstrasse 129, Dübendorf CH-8600, Switzerland
[§]Institut des Sciences et Ingénierie Chimiques, Ecole Polytechnique Fédérale de Lausanne (EPFL), Lausanne 1015, Switzerland

Supporting Information

ABSTRACT: Understanding the chemistry of colloidal quantum dots (QDs) is primarily hampered by the lack of analytical methods to selectively and discriminately probe the QD core, QD surface and capping ligands. Here, we present a general concept for studying a broad range of QDs such as CdSe, CdTe, InP, PbSe, PbTe, $CsPbBr_3$, etc., capped with both organic and inorganic surface capping ligands, through dynamic nuclear polarization (DNP) surface enhanced NMR spectroscopy. DNP can enhance NMR signals by factors of 10−100, thereby reducing the measurement times by 2−4 orders of magnitude. 1D DNP enhanced spectra acquired in this way are shown to clearly distinguish QD surface atoms from those of the QD core, and environmental effects such as oxidation. Furthermore, 2D NMR correlation experiments, which were previously inconceivable for QD surfaces, are demonstrated to be readily performed with DNP and provide the bonding motifs between the QD surfaces and the capping ligands.

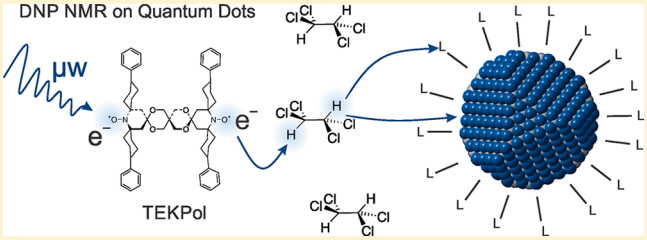

INTRODUCTION

Colloidal semiconductor nanocrystals, commonly referred to as quantum dots (QDs), exhibit size-tunable optical and electronic properties and have become important as luminescent labels in life sciences[1,2] and as building blocks for optoelectronic devices (solid-state lighting, photovoltaics, photodetectors and electronic circuitry).[3,4] QDs are complex entities comprising an inorganic crystalline core, surface atoms and surface capping ligands.[5] Adjustments of the QD surface chemistry control the optical properties of individual QDs as well as the charge and the energy transfer in assemblies of QDs, and allow for their integration into solid-state devices and versatile biofunctionalization. Importantly, QDs are highly dynamic and reactive objects, in both their core regions (e.g., with polymorphism, and rapid chemical transformations via oxidation, reduction, galvanic or ion-exchange, or self-purification from impurity atoms, etc.) and at their surfaces (e.g., surface reconstruction, ligand adsorption−desorption, etc). It is therefore not surprising that structural characterization and the atomistic description of QDs remains a formidable challenge. In principle, nuclear magnetic resonance (NMR) spectroscopy would be the method of choice because of its ability to characterize molecules, solids, surfaces and interfaces. Both solid-state magic-angle spinning nuclear magnetic resonance (MAS NMR) and solution NMR investigations of sub-10 nm colloidal QDs (CdSe, CdTe, InP and PbSe, etc.) have provided information about the internal structure of the QD cores[6−9] and about the organic ligand capping, including the QD-ligand-binding equilibria in the liquid state.[9−13] However, both approaches have intrinsic limitations with respect to the chemistry of QDs. Solution NMR provides accurate information about the structure and binding equilibria of molecular species such as QD capping ligands, but is essentially blind to surface-bound ligands due to their slow and nonuniform tumbling. In the solid state, direct excitation MAS NMR records signal from all species present in the sample, with the principle possibility to yield insight specific to the atomic structure of the QD surface and capping ligands via surface selective cross-polarization MAS (CPMAS) experiments.[14] However, CPMAS experiments on QDs are highly challenging due to the low concentrations of surface sites, the residual ligand dynamics that reduce heteronuclear ^1H-X dipolar couplings,[7] and most importantly, the generally poor sensitivity of NMR spectroscopy. From the QD chemistry point of view, NMR characterization should ideally be carried out directly on colloidal dispersions of QDs to rule out the effects of the isolation and purification procedures on the surface composition and surface coverage of the ligands. This challenge becomes even more daunting when considering that pristine QD colloids contain only milligram quantities of QDs, and the surface atoms and the stabilizing ligands constitute an even smaller fraction of the sample. To become practically useful,

Received: September 8, 2015
Published: October 16, 2015

DOI: 10.1021/jacs.5b09248
J. Am. Chem. Soc. 2015, 137, 13964−13971

solid-state NMR of dispersed colloids of QDs requires orders of magnitude increase in the measured signal.

In the past 20 years, *in situ* high-field dynamic nuclear polarization (DNP) enhanced MAS NMR spectroscopy has become an extremely powerful method to enhance NMR signals via microwave (μw) induced polarization transfer from unpaired electrons of a radical polarizing agent to nuclear spins.[15,16] With typical enhancement factors (ε) of 10−100, and corresponding shortening of the measurement times by 2−4 orders of magnitude ($\propto \varepsilon^2$), DNP enhanced NMR experiments may open new avenues for studying inorganic materials containing unreceptive NMR nuclei, such as QDs. Indeed, in the recent years, DNP enhanced NMR studies, exploiting unreceptive NMR nuclei such as ^{13}C, ^{15}N, ^{17}O, ^{29}Si, ^{59}Co, ^{119}Sn, have focused on inorganic surfaces and surface-bound molecules, providing enhanced spectra from surface atoms, including subsurface atomic layers of the material.[17−27] DNP surface enhanced NMR spectroscopy should thus be uniquely suited for colloidal QDs, which are usually just 3−10 nm in size and have high surface areas, and therefore can be polarized as a whole, allowing simultaneous and discriminative studies of the QD cores, surfaces and capping ligands, all in colloidal solutions, and without the need for invasive isolation and purification procedures. Virtually all known colloidal QD materials and their organic and inorganic ligand capping layers contain NMR active nuclei that potentially can benefit from DNP enhancement, including spin 1/2 nuclei (^{31}P, ^{77}Se, $^{111/113}$Cd, ^{115}In, $^{117/119}$Sn, ^{125}Te, ^{207}Pb, etc.) and also quadrupolar nuclei (nuclear spin >1/2, ^{133}Cs, ^{115}In, ^{17}O, ^{67}Zn, etc).

Here, we demonstrate how DNP enhanced NMR can provide unprecedented information about the structure of colloidal QDs, kept in the original colloidal state in the amount of just few milligrams. We obtain high signal enhancement factors of up to 80, corresponding to gains in acquisition times up to a factor 6400. Such efficient polarization results from the homogeneous dispersion of biradical polarizing agents and QDs in mesoporous silica (meso-SiO_2) and is readily obtained for all common QD materials such as CdSe, CdTe, InP, PbSe, PbTe, and $CsPbBr_3$, and stabilized by all kinds of surface functionalities (inorganic or organic, charge and steric stabilization) and dispersed in any suitable polar or apolar solvent. New insights specific to the structure of QDs were obtained with DNP enhanced 1D NMR spectra. For a canonical QD system, CdSe QDs, we present the first direct evidence for the core−shell CdSe−CdX_2 (X = oleate, phosphonate) morphology, by resolving bulk and surface Cd and Se atoms with ^{113}Cd and ^{77}Se DNP enhanced spectra. Similarly, InP QDs are seen to exhibit clearly resolvable core and surface ^{31}P DNP enhanced signals. ^{125}Te DNP NMR spectra point to massive differences between CdTe and PbTe QDs. CdTe QDs are seen to remain unoxidized even upon prolonged storage at ambient air, whereas PbTe QDs are found to comprise exclusively Te-oxide species at their surfaces, even with cautious air-free handling. To show new horizons for unreceptive quadrupolar nuclei, we show DNP enhancements of ^{133}Cs NMR spectra from perovskite $CsPbBr_3$ QDs. Previously inconceivable 2D correlation experiments can also be readily accomplished owing to strong signal enhancements, as demonstrated here for CdSe QDs with a 2D dipolar-HMQC ^{13}C−^{111}Cd correlation spectrum, which reveals the identity of Cd atoms to which carboxylate ligands bind as a single surface moiety.

EXPERIMENTAL SECTION

Synthesis of QDs. Organic-capped InP, W-CdSe, ZB-CdSe, PbSe, PbTe, CdTe QDs were synthesized and purified according to previously reported protocols, with slight modifications as detailed in Supporting Information. Care was taken to remove excess of ligands in the colloidal solutions used for DNP NMR experiments. Inorganic capped InP-S^{2-} and CdSe-Se^{2-} QDs were prepared via ligand-exchange reactions, as described by Nag et al.[28]

Conventional Solid-State MAS NMR Experiments. Solid-state NMR experiments at ambient conditions were performed on two Bruker spectrometers (11.7 and 17.6 T) equipped with 2.5 mm and 4 mm two-channel solid-state probe heads and Avance III consoles, while spinning between 0.6 and 20 kHz. Low temperature experiments were conducted on a commercial 14.1 T Bruker instrument equipped with an Avance III console and a double resonance 3.2 mm low temperature MAS probe using MAS spinning of 10 kHz. Chemical shifts were referenced to 85% H_3PO_4 in H_2O (^{31}P), Me_2Se (^{77}Se), Me_2Cd (^{113}Cd) and 0.1 M aqueous CsCl (^{133}Cs).

DNP Surface Enhanced Experiments. DNP NMR spectra were acquired on two Bruker DNP NMR spectrometers (9.4 and 14.1 T) equipped with Avance I and III consoles, and 263 and 395 GHz gyrotron microwave sources, respectively.[29] Double and triple 3.2 mm low temperature MAS probes were used in combination with 3.2 mm sapphire rotors.[29] For DNP NMR experiments, 1−4 mg of QDs were dispersed in 15−20 μL solution of biradical (16 mM TEKPol in TCE or 8 mM AMUPol in DMSO-d^6/H_2O/D_2O). This QD-biradical solution was either loaded directly into the rotor for reference experiments without meso-SiO_2 or, for one-step filling method, the meso-SiO_2 powder was impregnated with the QD-biradical solution on a watch glass, then transferred into a rotor. The mass ratio of meso-SiO_2 to QDs has been optimized for each system, as illustrated for MSU-H meso-SiO_2 and InP QDs in Figure S2. In a two-step method, the QD dispersion was first impregnated into the meso-SiO_2 host, and dried, followed by impregnation of the biradical solution, aiming at the same overall amounts of QDs and biradicals as in one-step method. Chemical shifts were referenced to Me_4Si (^{1}H, ^{13}C), 85% H_3PO_4 in H_2O (^{31}P), Me_2Se (^{77}Se), Me_2Cd ($^{111/113}$Cd), Me_2Te (^{125}Te), 0.1 M CsCl in H_2O (^{133}Cs). See the Supporting Information for further details on NMR measurements and sample preparation.

RESULTS AND DISCUSSION

DNP Enhanced NMR of QDs Using Meso-SiO_2 Matrix. The basic principle of DNP enhanced NMR experiments on colloidal QDs is outlined in Figure 1: the paramagnetic polarizing agent (here a nitroxide biradical) is dispersed in a suitable solvent (here TCE) and then brought into contact with the sample. Microwave (μw) irradiation transfers the polarization of the electron spins to the protons of the solvent and of other proton-containing molecular species residing at the QD surface. The enhanced proton polarization is then transferred through a CP step[30] to the desired heteronuclei. For QDs, the range of this transfer from the surface is such that nuclei residing in the capping ligands, the QD surface, or even the QD core are hyper-polarized.

However, *in situ* DNP NMR experiments are conducted at rather low temperatures, typically around 100 K to slow nuclear and electron relaxation.[15,16,31] In addition to the DNP effect, thermal (Boltzmann) enhancement of the NMR signal potentially contributes a factor 2.8 to the sensitivity at 100 K as compared to room temperature (RT). *The straightforward approach of mixing solutions of QDs and biradicals has proven to yield little or no enhancement.* This is because colloidal dispersions of QDs usually aggregate and precipitate upon

DOI: 10.1021/jacs.5b09248
J. Am. Chem. Soc. 2015, 137, 13964−13971

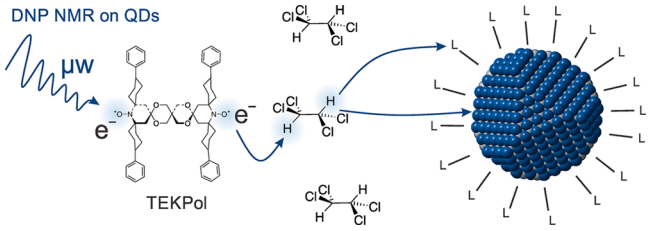

Figure 1. Schematics of the DNP surface enhanced NMR experiment for colloidal QDs. When the sample is irradiated with monochromatic microwaves (from a gyrotron source, here 263 or 395 GHz, depending upon magnetic field of the NMR spectrometer), the polarization of the unpaired electron spins of the biradical is transferred to the protons of the solvent and then relayed to the protons of the ligand by spin diffusion. CP is then used to transfer DNP enhanced ^{1}H polarization to the nuclei of interest in the capping ligand layer or to the heteronuclei of the QD surface or QD core. Alternative pathways, omitted for clarity, are also possible, such as direct polarization transfer from the biradical to the protons of the ligand. The depth of excitation in the QD depends on the nuclei, and the CP contact time (for details of the pulse sequences used see Figure S1), allowing either signal from preferentially the uppermost surface or excitation into the subsurface layers, as discussed in the main text. L stands for organic and/or inorganic capping ligands such as oleate, myristate, oleylamine, phosphonate, sulfide, selenide, etc. A 3 nm zinc-blende CdSe QD is shown as a model QD. 1,1,2,2-Tetrachloroethane (TCE) is a known suitable DNP polarizing medium, and TEKPol is a state of the art DNP polarizing agent.[32,33]

cooling, or even at room temperature in some cases, leading to phase separation from the biradical polarizing agent, and obliteration of the DNP effect. This aggregation can be clearly observed visually by placing concentrated QD colloids, with or without added biradicals, into a freezer at −40 °C. Importantly, due to the small size of the QDs (<10 nm), the voids within the aggregates are possibly too small to allow easy access for the relatively large polarizing molecules, and are mainly filled by the 1.5−2.5 nm-long surface ligands of QDs.

To solve this problem, here we introduce meso-SiO_2 (3−250 nm pore sizes) as a host matrix. The meso-SiO_2 is impregnated with a solution containing both the QDs and the biradicals, thereby maintaining homogeneity of the QD-biradical mixtures in an environment similar to the native chemical environment of colloidal QDs. Inexpensive, commercially available samples of nonfunctionalized meso-SiO_2 were used throughout this study. Importantly, the meso-SiO_2 is highly porous (71% porous volume for MSU-H with 7 nm pore size), meaning that the dilution factor is no higher than 1.5 (close to experimentally observed, as discussed below). Furthermore, sequential filling of the pores of meso-SiO_2 first with QDs and then with polarizing agent allows, for instance, study of highly charged inorganic-capped QDs with hydrophobic biradicals and vice versa.

Myristate-Capped InP QDs. Our initial DNP surface enhanced NMR experiments on QDs focused on myristate-capped InP QDs since ^{31}P is a highly receptive NMR nucleus, enabling the rapid optimization of sample preparation protocols. Owing to the presence of organic or inorganic capping ligand on their surfaces, 3−10 nm QDs form thermodynamically stable colloidal solutions at ambient temperatures (Figure 2a). For DNP NMR, the sample is usually loaded into a rotor at RT, and then transferred to the precooled DNP NMR probe where it is quickly frozen upon cooling to 100 K. In numerous attempts to obtain DNP surface enhanced NMR spectra of QDs simply by adding biradical solutions to concentrated QD colloids, we usually observed rather small DNP enhancement factors (ε < 5) for InP QDs (Figure 2b,d) and no enhancement for all other QD samples, in all cases due to aggregation and phase separation of QDs. On the contrary, as shown in Figure 2e, when the same colloidal

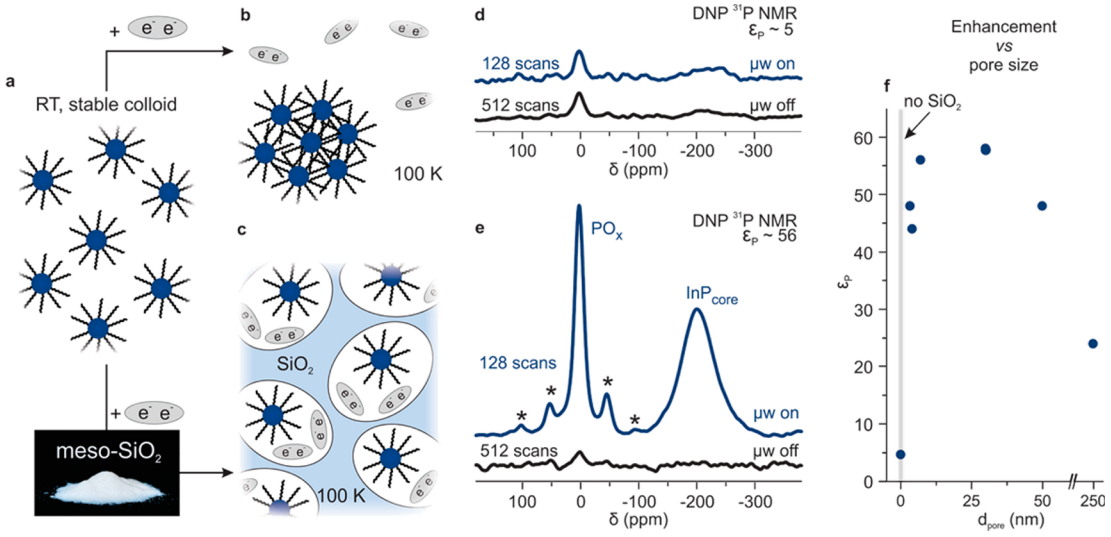

Figure 2. Effect of a meso-SiO_2 matrix on the success of DNP surface enhanced NMR experiments on colloidal myristate-capped 3 nm InP QDs. (a) At RT, the colloidal solution of organic-ligand capped QDs is fully thermodynamically stable, often up to concentrations of 30 wt % in tetrachloroethane. This solution is then mixed with the biradical polarizing agent TEKPol, retaining colloidal stability. (b) In the absence of meso-SiO_2, cooling to the measurement temperature of 100 K induces aggregation of QDs and phase separation from biradicals, an effect that is easily reversed upon warming the sample after withdrawal from the cooled DNP NMR probe and which thus often goes unnoticed. (c) The pores of meso-SiO_2 can fully (smaller pores) or partially (large pores) limit the aggregation. Consequently, (d) no or very low DNP enhancements are obtained in the absence of meso-SiO_2, while (e) reproducibly high enhancement factors between 60 and 80 are obtained for surface PO_x signal with meso-SiO_2. In (e), spinning sidebands are marked by asterisks. Panel f shows the DNP enhancements obtained for InP QD-TEKPol-TCE solutions with varying pore size of the meso-SiO_2. All experiments used 1−4 mg of InP QDs per sample.

DOI: 10.1021/jacs.5b09248
J. Am. Chem. Soc. 2015, 137, 13964−13971

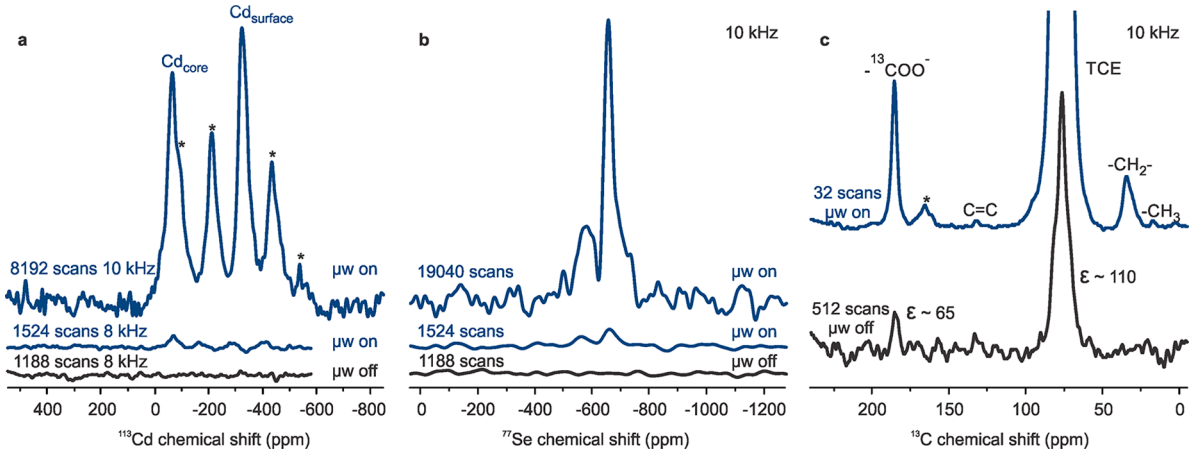

Figure 3. DNP surface enhanced NMR of oleate-capped 4 nm ZB-CdSe QDs. Spectra for both the QD core (^{113}Cd and ^{77}Se, a and b) and ligand (^{13}C, c) were acquired and DNP enhancements were obtained for all nuclei. The spinning side bands are marked by asterisks. Isotropic peaks and spinning sidebands were distinguished by varying the MAS frequency, Figure S7. $\delta(^{77}\text{Se})$ is referenced to Me_2Se, $\delta(^{13}\text{C})$ to Me_4Si, $\delta(^{113}\text{Cd})$ to Me_2Cd (for more discussion of ^{111}Cd/^{113}Cd δ-scale, see Supporting Information Table S1).

solution is impregnated into commercial powders of meso-SiO_2, high DNP enhancement factors of up to 80 can be obtained. Overall, with the QD colloid/biradical/meso-SiO_2 system, an absolute QD signal enhancement by a factor of 51 is obtained by comparison to rotor filled with frozen QD colloid only, clearly outweighing the diluting effect of the added meso-SiO_2 material and possible effects from the faster relaxation due to proximity of paramagnetic biradical (Figure 2c,e and Figure S2, including detailed comparison of enhancements for various sample formulations).

^{31}P DNP NMR spectra of 3 nm InP QDs clearly illustrate the high enhancements for signals at 0−10 ppm, assigned to surface PO_x species.[34,35] Furthermore, a large portion of the InP QD core is also enhanced, with a very broad peak centered at −200 ppm. The intensity of the surface and core QD NMR signals depend on the contact time set in the CP pulse sequence (Figure S3), consistent with previous conventional solid-state NMR experiments on InP QDs.[35] As expected, conventional single-pulse MAS NMR spectra taken from dried powders of same InP QDs mainly show signals from the QD core (Figure S4), highlighting the utility of DNP for obtaining surface-selective information.

We then evaluated the effect of pore size of meso-SiO_2 on the DNP enhancement of the QDs, as presented for the PO_x-signal from myristate-capped InP QDs in Figure 2f. First, we should note that each meso-SiO_2 sample has a distribution of pore sizes, around the one indicated as a nominal mean pore size. Thus, the 3.3 nm pore meso-SiO_2 with the smallest pore size has in fact a relatively broad pore size distribution in the 1−8 nm range and, therefore, can uptake large quantities of 3−4 nm QDs. The average population of QDs in meso-pores can vary from less than one-per-pore to as high as 20 QDs-per-pore (i.e., by placing a 300 mg/mL dispersion of the smallest 3 nm InP QDs, with a 2 nm-thick ligand shell, into 50 nm large spherical pores). Even if aggregation occurs in the latter case, the single aggregate size is still small enough to expose nearly all QDs to the effects of the biradical polarizing agent. A noticeable decrease in the enhancement factors can be found for all studied QDs only at extremely large pore sizes, above 100 nm, that allow aggregates sufficiently large to exclude a substantial fraction from the biradical. In control experiments without meso-SiO_2, DNP enhancements of 5 are obtained. Another beneficial effect is the inhibition of solvent crystallization in meso-SiO_2. DNP experiments typically require glass forming solvents which prevent aggregation of radicals upon freezing.[19] Therefore, the use of meso-SiO_2 as a host for DNP experiments has the added benefit that it could allow for a broader range of solvents to be used.

CdSe QDs. After two decades of research, CdSe QDs have become a canonical QD material in academic research, and the first QD product commercialized for consumer electronics (Sony's LCD TV displays, 2013). Importantly, CdSe QDs can be deliberately obtained in two polymorphs: zinc-blende (ZB, cubic) or wurzite (WZ, hexagonal). CdSe QD surface chemistry has received a great deal of attention in recent years.[5,12,36,37] The current consensus is that nonoxidized carboxylate-capped ZB-CdSe QDs (and likely WZ-CdSe QDs) comprise a CdSe core and a labile layer of surface Cd-atoms bound to carboxylate or other X-type anionic ligands, e.g., a $CdSe_{core}(CdX_2)_{shell}$ model, and therefore, they are Cd-rich as a whole.[36,38] Similar conclusions were drawn for Pb-chalcogenide QDs.[36,39] Inspired by the ability to differentiate core and surface ^{31}P NMR signals in the InP QDs, we turned to oleate-capped ZB-CdSe QDs, containing two NMR-accessible elements ($^{111/113}$Cd and ^{77}Se), seeking to directly probe the prevailing $CdSe_{core}(CdX_2)_{shell}$ model. With DNP surface enhanced NMR, we observed a signal at −20 ppm from the QD core and a strong signal from Cd surface species at −317 ppm (Figure 3a). Both core and surface Cd signals exhibit an inhomogeneous line broadening of approximately 4000 Hz, which is considerably larger than that of bulk CdSe,[7] and likely arises from positional variations in electronic environments when moving from the surface to the core.[13,35,40] The NMR signal of the surface Cd atoms gives rise to an extensive manifold of spinning sidebands, which reflects a substantial chemical shift anisotropy of ca. 400 ppm and the lower symmetry about the surface Cd atoms. On the other hand the Cd core signal shows fewer sidebands, consistent with the more symmetric environment expected in the core. In agreement with our assignments, control single-pulse MAS NMR experiments only show signals from the ZB-CdSe QD core at −83 ppm (Figure S5). Previous direct excitation ^{113}Cd MAS NMR experiments did not study ZB-CdSe QDs, but found ^{113}Cd chemical shifts of −96 ppm in bulk WZ-CdSe,[41] −65

DOI: 10.1021/jacs.5b09248
J. Am. Chem. Soc. 2015, 137, 13964−13971

ppm in WZ-CdSe QDs,[7] and −46 ppm for nearly ZB-like 2 nm CdSe nanoclusters[14] (all values are converted to a chemical shift scale with the chemical shift of Me_2Cd set to 0 ppm).

^{77}Se DNP surface enhanced NMR was also carried out for both ZB- and WZ-polymorphs, showing close chemical shifts of −579 and −654 ppm (Figure 3b) and −556 ppm (Figure S6), respectively. Two peaks in Figure 3b may point to the distinct contributions from the QD core (lower intensity peak) and (near) surface Se atoms, as was previously demonstrated for WZ-CdSe QDs.[14] The ^{77}Se chemical shifts obtained from DNP experiments on WZ-CdSe match the values previously reported for WZ-CdSe QDs using conventional ^{1}H−^{77}Se CPMAS.[6,14]

2D DNP Surface Enhanced Heteronuclear Correlation Spectra of CdSe QDs. Figure 3c shows that using the matrix-assisted approach, DNP enhanced ^{13}C-spectra from the surface-bound oleate ligands (e.g., ^{13}C-1-oleate; 27% ^{13}C-labeled on the carboxylate), with clearly resolved signals from all C atoms, can be acquired in less than 2 min (32 scans). This opens the possibility to acquire ^{13}C−X heteronuclear 2D correlation spectra within reasonable timeframes. Partial ^{13}C-labeling of the carboxylate carbon was employed in order to help in collecting a DNP enhanced ^{13}C−^{111}Cd 2D dipolar heteronuclear multiple-quantum coherence (D-HMQC) correlation spectrum of oleate-capped ZB-CdSe QDs (Figure 4). Here ^{111}Cd was used rather than the more sensitive ^{113}Cd since the triple resonance probe could not be configured in ^{1}H/^{13}C/^{113}Cd mode. Such experiments yield correlations between ^{13}C and ^{111}Cd heteronuclei that are close in space. The 2D spectrum (obtained overnight) shows clear correlations between carboxylate and Cd atoms at the QD surface, providing direct evidence for the $CdSe_{core}(CdX_2)_{shell}$ model. This model was previously inferred indirectly by observing the ligand absorption/displacement dynamics with ^{1}H NMR.[36] On the basis of the signal-to-noise ratios of on/off ^{13}C-spectra, the acquisition time of non-DNP-enhanced 2D spectra would be prohibitively long, taking more than 1000 days.

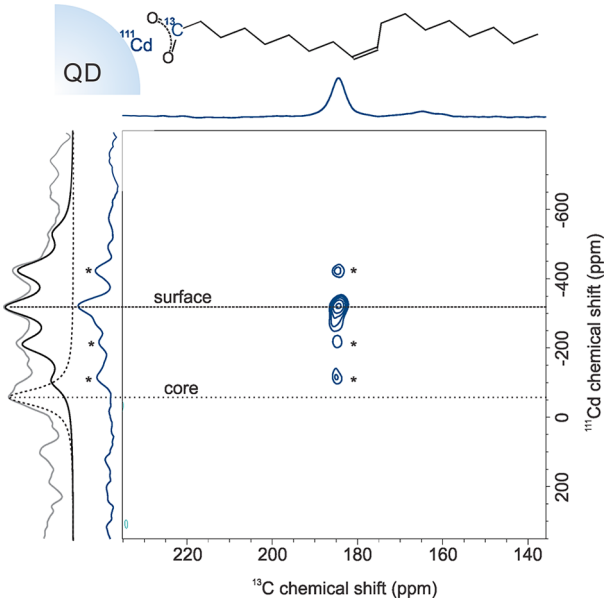

Figure 4. DNP enhanced D-HMQC spectrum correlating ^{13}C-1-oleate ligands and ^{111}Cd of ZB-CdSe. Projections of the 2D spectrum are shown in dark blue. A DNP NMR ^{111}Cd CPMAS spectrum acquired separately is shown in light gray. The isotropic shifts of the surface and core Cd-species identified before (Figure 3) are highlighted with solid and dotted black curves. The spinning sidebands are marked by asterisks. It is apparent that the Cd-species with signal at −317 ppm is directly binding to oleic acid. No correlation between the ^{111}Cd of the QD core (−20 ppm) and ^{13}C nuclei of the ligand was observed for the recoupling time used (3 ms). In control experiments, the DNP enhanced NMR spectrum of free $Cd(oleate)_2$ diluted in TCE is characterized by a single peak with chemical shift distinctly different from all Cd signals recorded from ZB-CdSe QDs (Figure S8). Here ^{111}Cd was used rather than the more sensitive ^{113}Cd since the triple resonance probe could not be configured in ^{1}H/^{13}C/^{113}Cd mode. First order rotary resonance recoupling (R^3) was employed.

Sequential Filling Method of Meso-SiO_2 for Inorganic-Capped and Air-Sensitive QDs. In the studies presented thus far, one-step filling of meso-SiO_2 with a QD-biradical mixture was sufficient to prevent phase separation. Furthermore, common long-chain ligand-capped QDs enjoy full compatibility and miscibility with apolar solvent-biradical mixtures previously optimized for DNP. Negative consequences were encountered when attempting the same approach for highly polar, charge-stabilized QDs, such as those capped with S^{2-} and Se^{2-} ions as inorganic ligands (in the form of K_2S and K_2Se). Such inorganic capping ligands are of strategic importance for integration of QDs into (opto)electronic devices due to the high charge carrier mobility they impart into QD solids.[42,43]

There are much fewer polar solvent-biradical mixtures which simultaneously solubilize charge-stabilized QDs and allow for efficient DNP enhancements. The only working example we identified so far is AMUPol in DMSO-d^6/H_2O/D_2O, which is suitable for studying chemically robust materials such as sulfide capped Sn/SnO_x nanocrystals.[22] Water in this mixture is required for efficient polarization transfer, but promotes hydrolysis and oxidation of sensitive QD materials. To circumvent these problems, a facile and versatile two-step method for filling the meso-SiO_2 matrix is presented in Figure 5. This method eliminates a tedious search for suitable compatible QD−solvent−radical combinations. First, impregnation of the meso-SiO_2 was done with a QD dispersion in any given type of solvent, polar or apolar, followed by the evaporation of the solvent to deposit the QDs in the meso-SiO_2. Second, the meso-SiO_2 filled with QDs was then impregnated with any other given (polar or apolar) biradical−solvent mixture. Hence, apolar solvent−biradical combinations can be used for enhancing NMR signals of highly polar inorganic-capped QDs, and vice versa. In the first case study, highly oxygen and moisture-sensitive selenide (Se^{2-}) capped CdSe QDs, prepared from oleate-capped QDs via a ligand-exchange reaction,[28] were deposited into meso-SiO_2 from formamide solution. Subsequent ^{77}Se DNP NMR with the TEKPol-TCE polarization mixture yields a spectrum with higher signal-to-noise ratio (Figure 5a, 3000 scans) than was obtained for carboxylate-capped CdSe NCs (Figure 3b). The ^{77}Se spectrum of CdSe-Se^{2-} QDs is, however, asymmetrically broader (see direct comparison in Figure S9), presumably due to contribution from the surface-bound Se^{2-} with a chemical shift only subtly different to the core Se nuclei. This conclusion is supported by the control experiments with unbound Se^{2-}, where the ^{77}Se chemical shifts of frozen solutions and powders of K_2Se were much further separated (by several hundred ppm, Figure S9).

More chemically robust sulfide (S^{2-}) inorganic-capped InP QDs are compatible with an AMUPol-DMSO-d^6/H_2O/D_2O polarizing mixture, allowing direct comparison between one-

DOI: 10.1021/jacs.5b09248
J. Am. Chem. Soc. 2015, 137, 13964−13971

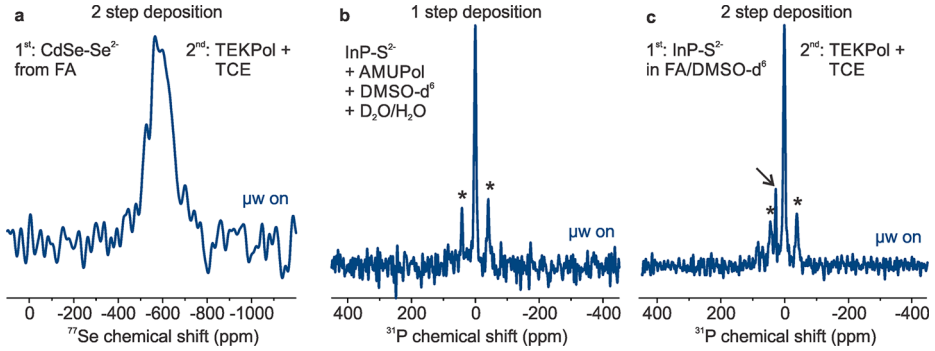

Figure 5. DNP surface enhanced NMR on air-sensitive and inorganic-capped QDs using sequential filling of meso-SiO_2 (two-step method). CdSe-Se^{2-} QDs are highly oxygen and moisture sensitive and could be studied only with two-step deposition method (a). InP-S^{2-} QDs have been deposited into silica pores by one (b) and two-step (c) procedures. The two-step procedure does not involve any water during preparation and yields an additional peak in the spectrum (indicated by an arrow), attributed to PO_xS_y species, absent in (b) due to full conversion into PO_x species. The spinning sidebands are marked by asterisks.

step and two-step filling methods. Similar DNP enhancement factors were obtained in both cases (Figure 5b,c), yet with a noticeable difference in the obtained ^{31}P NMR spectra. The ^{31}P CPMAS NMR spectrum from the two-step, water-free deposition features an additional peak (marked with an arrow in Figure 5c). Although the chemical identity of this signal is not fully clear, we can speculate that they are due to PO_xS_y surface species, which are otherwise fully oxidized and/or hydrolyzed in a water-based polarizing mixture.

Other Tested Systems, Concluding Remarks and outlook. So far precipitation of QDs to form powdered samples had remained the only practical option for solid-state NMR studies on QDs. Precipitation may change the chemical identity of the surface QD atoms and/or surface ligands. In this study, we have shown that meso-SiO_2-assisted DNP experiments allow for using colloidal dispersions of QDs directly for solid-state NMR spectroscopy to study QDs in an environment more similar to a dispersion. Owing to efficient proton DNP enhancements (ε_H = 40−80), absolute signals obtained with small sample amounts (1−4 mg of QDs per sample throughout this study) are always much greater than conventional MAS NMR signals from a rotor densely packed with large quantities of QDs (up to 100−200 mg). In fact, there are clear physical and hardware limits to scaling the MAS NMR signal by using larger sample quantities and larger rotors. Without DNP enhancement, acquisition of 1D CPMAS spectra from 1 to 2 mg of QDs would take months or even years. The matrix-assisted method enables acquisition of 2D spectra between heteronuclei in reasonable timeframes (hours instead of years) and allows a whole new plethora of studies to be carried out, such as directly probing metal−ligand binding at the QD surface (as shown here for Cd-oleate at the CdSe surface), and possibly intraligand and intra-QD local chemical structure. With a two-step sequential filling method, problems such as air and moisture sensitivity, solvent incompatibility and low solubility can be easily circumvented. With the advent of commercial DNP NMR spectrometers, and the active development of suitable biradical polarization transfer agents,[32,44] DNP enhanced NMR spectroscopy holds great promise to address various research problems in contemporary nanomaterials research. Meso-SiO_2 of appropriate pore size is also likely to be of great help for ensuring homogeneous DNP excitation of many other important analytes such as polymers, biomolecules, colloids, and coordination compounds, yet with minimal dilution effect.

Specific to the chemistry of QDs, DNP surface enhanced NMR yields signatures from the QD core, QD surface, and surface-bound ligands. For CdSe QDs as a case study, we were able for the first time to clearly distinguish Cd atoms from the QD core and QD surface, thanks to the tunable surface-selectivity of DNP. Hence strong evidence is obtained here in support of a $CdSe_{core}(CdX_2)_{shell}$ (X = oleate ligand) morphology of these QDs. Correspondingly, ^{77}Se spectra point to the gradient of chemical shifts within the QD core, rather than new surface species. Furthermore, large DNP enhancements permitted fast acquisition of ^{111}Cd-^{13}C 2D-correlation spectra within the surface Cd-carboxylate layer, directly determining ligand binding to the CdSe QD surface. Future studies will expand such analysis to shape and composition engineered CdSe nanostructures such as highly luminescent core−shell $CdSe/Cd_{1-x}Zn_xS$ QDs (x = 0−1).[45,46] or atomically flat Cd chalcogenide nanoplatelets[47] and nanorods.[48] For the later, preliminary experiments shown enhancement factors of up to 35 using 30−50 nm large pores of meso-SiO_2. Besides two detailed case studies, InP and CdSe QDs, we were also able to record DNP enhanced spectra for a variety of other important QD core materials in a short survey study (DNP enhanced nuclei in parentheses, see Figure S10): PbSe (^{77}Se), CdTe (^{125}Te), and PbTe (^{125}Te). For example, the DNP enhanced ^{125}Te solid-state NMR spectra illustrate large difference in stability with respect to oxidation of CdTe and PbTe QDs (Figure S10). We observe that PbTe QDs comprise exclusively Te-oxide species at their surfaces, even when freshly prepared and handled air-free, while CdTe QDs remain unoxidized upon long storage in air. These preliminary results pave the way toward new atomistic insights into the chemistry of these QDs in future studies. In another trial, we deposited nanocrystalline $CsPbBr_3$, perovskite-type highly luminescent semiconductors[49] into pores of meso-SiO_2 and recorded DNP enhanced spectra of ^{133}Cs (Figure S11), for the first time for this nucleus to the best of our knowledge. This result highlights the utility and future prospects of DNP also for nanomaterials containing quadrupolar nuclei.

■ ASSOCIATED CONTENT

Supporting Information

The Supporting Information is available free of charge on the ACS Publications website at DOI: 10.1021/jacs.5b09248.

DOI: 10.1021/jacs.5b09248
J. Am. Chem. Soc. 2015, 137, 13964−13971

Materials, methods, supporting Figures S1−S11 and Table S1 and additional explanations (PDF)

AUTHOR INFORMATION

Corresponding Authors

*mvkovalenko@ethz.ch
*ccoperet@ethz.ch
*lyndon.emsley@epfl.ch

Notes

The authors declare no competing financial interest.

ACKNOWLEDGMENTS

M.V.K. acknowledges financial support from the European Union through the FP7 (ERC Starting Grant NANOSOLID, GA No. 306733) and L.E. acknowledges support from ERC Advanced Grant No. 320860. René Verel and Maxence Valla are acknowledged for their help at the NMR facility at ETH Zurich. Davisil silica matrices with ≥50 nm pore sizes were gifts of GRACE. Georgian Nedelcu is acknowledged for providing InP QDs, Tanja Zünd for CdTe QDs, Maria Ibáñez Sabate for PbTe QDs, David Trummer for $CsPbBr_3$ nanostructures, and Indre Thiel for supplying meso-SiO_2 with 3.3 nm pore size.

REFERENCES

(1) Chen, O.; Riedemann, L.; Etoc, F.; Herrmann, H.; Coppey, M.; Barch, M.; Farrar, C. T.; Zhao, J.; Bruns, O. T.; Wei, H.; Guo, P.; Cui, J.; Jensen, R.; Chen, Y.; Harris, D. K.; Cordero, J. M.; Wang, Z.; Jasanoff, A.; Fukumura, D.; Reimer, R.; Dahan, M.; Jain, R. K.; Bawendi, M. G. *Nat. Commun.* **2014**, *5*, 5093.

(2) Medintz, I. L.; Stewart, M. H.; Trammell, S. A.; Susumu, K.; Delehanty, J. B.; Mei, B. C.; Melinger, J. S.; Blanco-Canosa, J. B.; Dawson, P. E.; Mattoussi, H. *Nat. Mater.* **2010**, *9*, 676−684.

(3) Talapin, D. V.; Lee, J.-S.; Kovalenko, M. V.; Shevchenko, E. V. *Chem. Rev.* **2010**, *110*, 389−458.

(4) Kim, D. K.; Lai, Y.; Diroll, B. T.; Murray, C. B.; Kagan, C. R. *Nat. Commun.* **2012**, *3*, 1216.

(5) Owen, J. *Science* **2015**, *347*, 615−616.

(6) Lovingood, D. D.; Achey, R.; Paravastu, A. K.; Strouse, G. F. *J. Am. Chem. Soc.* **2010**, *132*, 3344−3354.

(7) Ratcliffe, C. I.; Yu, K.; Ripmeester, J. A.; Badruz Zaman, M.; Badarau, C.; Singh, S. *Phys. Chem. Chem. Phys.* **2006**, *8*, 3510−3519.

(8) Abraham, A.; Mihaliuk, E.; Kumar, B.; Legleiter, J.; Gullion, T. *J. Phys. Chem. C* **2010**, *114*, 18109−18114.

(9) Yesinowski, J. P. *Top. Curr. Chem.* **2012**, *306*, 229−312.

(10) Sachleben, J. R.; Colvin, V.; Emsley, L.; Wooten, E. W.; Alivisatos, A. P. *J. Phys. Chem. B* **1998**, *102*, 10117−10128.

(11) Sachleben, J. R.; Wooten, E. W.; Emsley, L.; Pines, A.; Colvin, V. L.; Alivisatos, A. P. *Chem. Phys. Lett.* **1992**, *198*, 431−436.

(12) Hens, Z.; Martins, J. C. *Chem. Mater.* **2013**, *25*, 1211−1221.

(13) Cadars, S.; Smith, B. J.; Epping, J. D.; Acharya, S.; Belman, N.; Golan, Y.; Chmelka, B. F. *Phys. Rev. Lett.* **2009**, *103*, 136802.

(14) Berrettini, M. G.; Braun, G.; Hu, J. G.; Strouse, G. F. *J. Am. Chem. Soc.* **2004**, *126*, 7063−7070.

(15) Maly, T.; Debelouchina, G. T.; Bajaj, V. S.; Hu, K.-N.; Joo, C.-G.; Mak-Jurkauskas, M. L.; Sirigiri, J. R.; van der Wel, P. C. A.; Herzfeld, J.; Temkin, R. J.; Griffin, R. G. *J. Chem. Phys.* **2008**, *128*, 052211.

(16) Ni, Q. Z.; Daviso, E.; Can, T. V.; Markhasin, E.; Jawla, S. K.; Swager, T. M.; Temkin, R. J.; Herzfeld, J.; Griffin, R. G. *Acc. Chem. Res.* **2013**, *46*, 1933−1941.

(17) Lesage, A.; Lelli, M.; Gajan, D.; Caporini, M. A.; Vitzthum, V.; Miéville, P.; Alauzun, J.; Roussey, A.; Thieuleux, C.; Mehdi, A.; Bodenhausen, G.; Coperet, C.; Emsley, L. *J. Am. Chem. Soc.* **2010**, *132*, 15459−15461.

(18) Lelli, M.; Gajan, D.; Lesage, A.; Caporini, M. A.; Vitzthum, V.; Mieville, P.; Heroguel, F.; Rascon, F.; Roussey, A.; Thieuleux, C.; Boualleg, M.; Veyre, L.; Bodenhausen, G.; Coperet, C.; Emsley, L. *J. Am. Chem. Soc.* **2011**, *133*, 2104−2107.

(19) Rossini, A. J.; Zagdoun, A.; Lelli, M.; Lesage, A.; Copéret, C.; Emsley, L. *Acc. Chem. Res.* **2013**, *46*, 1942−1951.

(20) Sangodkar, R. P.; Smith, B. J.; Gajan, D.; Rossini, A. J.; Roberts, L. R.; Funkhouser, G. P.; Lesage, A.; Emsley, L.; Chmelka, B. F. *J. Am. Chem. Soc.* **2015**, *137*, 8096−8112.

(21) Perras, F. A.; Kobayashi, T.; Pruski, M. *J. Am. Chem. Soc.* **2015**, *137*, 8336−8339.

(22) Protesescu, L.; Rossini, A. J.; Kriegner, D.; Valla, M.; de Kergommeaux, A.; Walter, M.; Kravchyk, K. V.; Nachtegaal, M.; Stangl, J.; Malaman, B.; Reiss, P.; Lesage, A.; Emsley, L.; Copéret, C.; Kovalenko, M. V. *ACS Nano* **2014**, *8*, 2639−2648.

(23) Corzilius, B.; Michaelis, V. K.; Penzel, S. A.; Ravera, E.; Smith, A. A.; Luchinat, C.; Griffin, R. G. *J. Am. Chem. Soc.* **2014**, *136*, 11716−11727.

(24) Wolf, P.; Valla, M.; Rossini, A. J.; Comas-Vives, A.; Núñez-Zarur, F.; Malaman, B.; Lesage, A.; Emsley, L.; Copéret, C.; Hermans, I. *Angew. Chem., Int. Ed.* **2014**, *53*, 10179−10183.

(25) Akbey, Ü.; Altin, B.; Linden, A.; Özçelik, S.; Gradzielski, M.; Oschkinat, H. *Phys. Chem. Chem. Phys.* **2013**, *15*, 20706−20716.

(26) Lafon, O.; Thankamony, A. S. L.; Rosay, M.; Aussenac, F.; Lu, X.; Trebosc, J.; Bout-Roumazeilles, V.; Vezin, H.; Amoureux, J.-P. *Chem. Commun.* **2013**, *49*, 2864−2866.

(27) Zagdoun, A.; Rossini, A. J.; Gajan, D.; Bourdolle, A.; Ouari, O.; Rosay, M.; Maas, W. E.; Tordo, P.; Lelli, M.; Emsley, L.; Lesage, A.; Coperet, C. *Chem. Commun.* **2012**, *48*, 654−656.

(28) Nag, A.; Kovalenko, M. V.; Lee, J.-S.; Liu, W.; Spokoyny, B.; Talapin, D. V. *J. Am. Chem. Soc.* **2011**, *133*, 10612−10620.

(29) Rosay, M.; Tometich, L.; Pawsey, S.; Bader, R.; Schauwecker, R.; Blank, M.; Borchard, P. M.; Cauffman, S. R.; Felch, K. L.; Weber, R. T.; Temkin, R. J.; Griffin, R. G.; Maas, W. E. *Phys. Chem. Chem. Phys.* **2010**, *12*, 5850−5860.

(30) Pines, A.; Gibby, M.; Waugh, J. *J. Chem. Phys.* **1973**, *59*, 569−590.

(31) Hall, D. A.; Maus, D. C.; Gerfen, G. J.; Inati, S. J.; Becerra, L. R.; Dahlquist, F. W.; Griffin, R. G. *Science* **1997**, *276*, 930−932.

(32) Zagdoun, A.; Casano, G.; Ouari, O.; Schwaerzwalder, M.; Rossini, A. J.; Aussenac, F.; Yulikov, M.; Jeschke, G.; Coperet, C.; Lesage, A.; Tordo, P.; Emsley, L. *J. Am. Chem. Soc.* **2013**, *135*, 12790−12797.

(33) Matsuki, Y.; Maly, T.; Ouari, O.; Karoui, H.; Le Moigne, F.; Rizzato, E.; Lyubenova, S.; Herzfeld, J.; Prisner, T.; Tordo, P.; Griffin, R. G. *Angew. Chem., Int. Ed.* **2009**, *48*, 4996−5000.

(34) Cros-Gagneux, A.; Delpech, F.; Nayral, C.; Cornejo, A.; Coppel, Y.; Chaudret, B. *J. Am. Chem. Soc.* **2010**, *132*, 18147−18157.

(35) Tomaselli, M.; Yarger, J. L.; Bruchez, M.; Havlin, R. H.; deGraw, D.; Pines, A.; Alivisatos, A. P. *J. Chem. Phys.* **1999**, *110*, 8861−8864.

(36) Anderson, N. C.; Hendricks, M. P.; Choi, J. J.; Owen, J. S. *J. Am. Chem. Soc.* **2013**, *135*, 18536−18548.

(37) Kovalenko, M. V.; Manna, L.; Cabot, A.; Hens, Z.; Talapin, D. V.; Kagan, C. R.; Klimov, V. I.; Rogach, A. L.; Reiss, P.; Milliron, D. J.; Guyot-Sionnnest, P.; Konstantatos, G.; Parak, W. J.; Hyeon, T.; Korgel, B. A.; Murray, C. B.; Heiss, W. *ACS Nano* **2015**, *9*, 1012−1057.

(38) Fritzinger, B.; Capek, R. K.; Lambert, K.; Martins, J. C.; Hens, Z. *J. Am. Chem. Soc.* **2010**, *132*, 10195−10201.

(39) Zherebetskyy, D.; Scheele, M.; Zhang, Y.; Bronstein, N.; Thompson, C.; Britt, D.; Salmeron, M.; Alivisatos, P.; Wang, L.-W. *Science* **2014**, *344*, 1380−1384.

(40) Thayer, A. M.; Steigerwald, M. L.; Duncan, T. M.; Douglass, D. C. *Phys. Rev. Lett.* **1988**, *60*, 2673−2676.

(41) Nolle, A. *Z. Naturforsch., A: Phys. Sci.* **1978**, *33*, 666−671.

(42) Jang, J.; Liu, W.; Son, J. S.; Talapin, D. V. *Nano Lett.* **2014**, *14*, 653−662.

(43) Lee, J.-S.; Kovalenko, M. V.; Huang, J.; Chung, D. S.; Talapin, D. V. *Nat. Nanotechnol.* **2011**, *6*, 348−352.

(44) Kiesewetter, M. K.; Corzilius, B.; Smith, A. A.; Griffin, R. G.; Swager, T. M. *J. Am. Chem. Soc.* **2012**, *134*, 4537−4540.

DOI: 10.1021/jacs.5b09248
J. Am. Chem. Soc. 2015, 137, 13964−13971

(45) Dang, C.; Lee, J.; Breen, C.; Steckel, J. S.; Coe-Sullivan, S.; Nurmikko, A. *Nat. Nanotechnol.* **2012**, *7*, 335−339.
(46) Chen, O.; Zhao, J.; Chauhan, V. P.; Cui, J.; Wong, C.; Harris, D. K.; Wei, H.; Han, H.-S.; Fukumura, D.; Jain, R. K.; Bawendi, M. G. *Nat. Mater.* **2013**, *12*, 445−451.
(47) Bouet, C.; Tessier, M. D.; Ithurria, S.; Mahler, B.; Nadal, B.; Dubertret, B. *Chem. Mater.* **2013**, *25*, 1262−1271.
(48) Robinson, R. D.; Sadtler, B.; Demchenko, D. O.; Erdonmez, C. K.; Wang, L.-W.; Alivisatos, A. P. *Science* **2007**, *317*, 355−358.
(49) Stoumpos, C. C.; Malliakas, C. D.; Peters, J. A.; Liu, Z.; Sebastian, M.; Im, J.; Chasapis, T. C.; Wibowo, A. C.; Chung, D. Y.; Freeman, A. J.; Wessels, B. W.; Kanatzidis, M. G. *Cryst. Growth Des.* **2013**, *13*, 2722−2727.

DOI: 10.1021/jacs.5b09248
J. Am. Chem. Soc. 2015, 137, 13964−13971